Heliyon 10 (2024) e31205

Contents lists available at ScienceDirect

Heliyon

journal homepage: www.cell.com/heliyon

Research article

Unveiling the anti-echinococcal efficacy of amide-based compounds: An *in-silico* and *in-vitro* study

V. Chauhan, Ph.D [a], U Farooq, Ph.D [b,*], M. Fahmi, DScD [c], Khan A, Ph.D [b], P. K. Tripathi, Ph.D [d]

[a] *Multi-Disciplinary Research Unit, Government Institute of Medical Sciences, Greater Noida, UP, 201310, India*
[b] *Department of Basic Oral Medicine and Allied Dental Sciences, Faculty of Dentistry, Taif University, Taif, Kingdom of Saudi Arabia*
[c] *Department of Restorative Dental Science, Faculty of Dentistry, Taif University, Taif, Kingdom of Saudi Arabia*
[d] *Department of Parasitology, Post Graduate Institute of Medical Education and Research, Chandigarh, 160012, India*

A R T I C L E I N F O

Keywords:
Amide-based compound
Anti-echinococcal
Cystic Echinococcosis
In-vitro
In-silico
Protoscoleces

A B S T R A C T

Cystic echinococcosis (CE) is a significant global public health concern, particularly in regions where livestock rearing is prevalent. Despite its impact on morbidity and mortality, CE has received insufficient attention compared to other neglected tropical diseases. The complexities in CE management arise from challenges in early detection, effective treatment, and parasite eradication. The present study addresses this gap by exploring innovative therapeutic approaches using amide-based compounds. In recent years, computational approaches and *in-vitro* studies have become prominent in neglected tropical disease drug discovery. Leveraging insights from previous studies on amide-based compounds with anti-parasitic potential, this study systematically designed, synthesized, and characterized a library of 30 amide compounds. The research integrated *in-silico* screening, molecular docking, and *in-vitro* experimentation to assess the anti-echinococcal potential of these compounds. The study identified five promising amide compounds, namely 3,5-dinitro-N-p-tolylbenzamide, N-p-tolyl-1-naphthamide, N-p-tolyl-4-(trifluoromethoxy)benzamide, 4-pentyl-N-p-tolylbenzamide, and 2,3,4,5,6-pentafluoro-N-p-tolylbenzamide, based on their docking scores. These compounds were synthesized and characterized through various spectroscopic techniques, confirming their structural integrity. The *in-vitro* cytotoxicity assay on HepG2 cell lines revealed varying degrees of cytotoxicity for the synthesized compounds. Notably, 4-pentyl-N-p-tolylbenzamide demonstrated the least cytotoxicity. Subsequent scolicidal activity assessments on *E. granulosus* protoscoleces demonstrated the potent protoscolicidal activity of N-p-tolyl-1-naphthamide, indicating its potential as an effective anti-echinococcal agent. Overall, this study presents a comprehensive exploration of amide-based compounds as potential therapeutic agents against CE. The findings contribute to the development of innovative strategies for CE treatment, addressing the urgent need for effective and safe drugs in managing this neglected tropical disease.

* Corresponding author. Department of Basic Oral Medicine and Allied Dental Sciences, Faculty of Dentistry, Taif University, Taif, Kingdom of Saudi Arabia.

E-mail addresses: varunc1784@gmail.com (V. Chauhan), umarfarooq@tudent.org (U. Farooq), mkfahmi@tudent.org (M. Fahmi), amirkhan@tudent.org (K. A), tripathi666@yahoo.com (P.K. Tripathi).

https://doi.org/10.1016/j.heliyon.2024.e31205
Received 11 February 2024; Received in revised form 12 May 2024; Accepted 13 May 2024
Available online 14 May 2024

1. Introduction

Cystic echinococcosis (CE), a chronic zoonotic parasitic disease caused by infection with larvae of *Echinococcus granulosus sensu lato (s.l.)*, is a significant global public health concern [1], especially in regions where livestock rearing is prevalent [2]. The incidence of CE ranges from 1/100,000 to 200/100,000 worldwide, posing substantial challenges to healthcare systems [3]. The fatality rate attributed to CE ranges approximately from 2 % to 4 %, although it can rise significantly under conditions of insufficient medical intervention and support. CE exhibits endemicity across the globe, presenting with minimal occurrence in Western Europe and escalating to notable levels in specific areas of central Asia and China [4]. This zoonotic disease affects humans as accidental intermediate hosts, primarily through the accidental ingestion of *E. granulosus* eggs discharged by dogs, leading to the formation of hydatid cysts in various organs, notably the liver and lungs [5,6]. Despite its considerable impact on morbidity and mortality, CE has received insufficient attention compared to other neglected tropical diseases. The complexities associated with CE management arise from challenges in early detection, effective treatment, and the eradication of the parasite [7]. Currently, the primary treatment for CE involves a combination of surgery and drug therapy; however, this approach carries risks of infection and recurrence during surgical intervention [8]. While pharmacological treatment can effectively reduce recurrence rates and improve surgical cure rates, the recommended drug, albendazole, is hindered by poor absorption, low bioavailability, and limited therapeutic efficacy [4]. Unfortunately, no new drugs have been developed to date, emphasizing the urgent need for innovative therapeutic approaches to address the challenges associated with CE treatment.

In recent years, computational approaches and *in-vitro* studies have gained prominence in drug discovery for neglected tropical diseases. Amide-based compounds have previously demonstrated anti-parasitic potential against various parasites, as documented by several research groups [9–11]. Leveraging these insights, the present study aimed to evaluate the anti-echinococcal potential of amide-based compounds through an integrated *in-silico* and *in-vitro* methodology. Employing state-of-the-art bioinformatics tools and advanced spectroscopic techniques, we systematically designed, synthesized, and characterized a library of amide compounds, opening new avenues for the development of innovative therapeutic strategies to combat CE.

2. Methodology

2.1. Ethical clearance

The study commenced following the approval granted by the Institutional Ethical Committee (IEC) of Shoolini University, Solan (HP), under reference number SUBMS/IEC/10/52.

2.2. Preparation of a library of ligands (amide-based compounds)

A collection of 30 amide-based compounds (ligands) was generated using Chemdraw 8.0 software [12]. The pdb files corresponding to these amides were crafted utilizing the online SMILES translator server (https://cactus.nci.nih.gov/translate/) and further structured in Pymol. Subsequently, the ligands underwent *in-silico* screening to predict their affinity towards the drug targets of *E. granulosus*. Various parameters, including the Lipinski rule of five, molecular volume, and Weiner index, were computed to assess the designed compounds using scfbio tool [13].

2.3. Selection of anti-echinococcal protein targets, modelling and molecular docking

The amino acid sequences corresponding to the selected drug targets, namely Aquaporin 4 (Na + channel), Kinase A, Fatty acid binding protein, and Glucose-6-phosphate-1-dehydrogenase, were retrieved from the NCBI database with the following IDs: EUB60918.1, EUB60795.1, Q02970.2, and EUB60927.1. To construct 3D models of these proteins, the I-Tasser server was employed [14]. Further, the models were refined by employing Galaxy refine server (https://galaxy.seoklab.org/cgi-bin/submit.cgi?type=REFINE). The identification of essential binding pockets on the receptor molecules (drug targets) was conducted using the Dogsite server [15]. This server employs a grid-based function prediction method, utilizing a Difference of Gaussian filter to detect potential pockets on the protein surface and segregating them into sub-pockets. Subsequently, molecular docking between the drug targets and amide-based compounds was executed through AutoDockVina [16].

2.4. Synthetic strategy of amides

The amides identified as potential anti-echinococcal molecules following docking analysis were synthesized and assessed for their *in-vitro* anti-echinococcal efficacy. In a two-necked round-bottom flask containing ketone, an equimolar mixture of p-toluidine and variously substituted acid chlorides was gradually added using a dropping funnel. The reaction mixture underwent reflux for 2–3 h at 40–45 °C, utilizing a nano molar quantity of silver nanoparticles (5–10 nM) as a catalyst, resulting in the formation of a dense precipitate. The amount of silver nanoparticles added in the synthesis process was determined based on a standardized protocol established in previous studies [17,18]. The reaction's completion was confirmed via thin-layer chromatography (TLC) using a solvent ratio of 1:1 (petroleum ether: ethyl acetate), revealing no reactant spots and a singular spot on the TLC plate. The newly formed reaction product was then extracted using diethyl ether and ethyl acetate, followed by drying over anhydrous Na_2SO_4 and concentration under a rotary evaporator. The purity of the synthesized benzamides was validated by column chromatography, displaying single spots.

Characterization of the synthesized compounds involved various spectroscopic techniques such as Ultra Violet (UV) spectroscopy, Infrared (IR) spectroscopy, Carbon-13 nuclear magnetic resonance (^{13}CNMR), and Proton nuclear magnetic resonance (^{1}HNMR), along with mass spectrometry (MS). Physico-chemical properties, including colour, physical state, retention factor (Rf value calculated from TLC), and melting point, were also documented.

2.5. Purification & characterization of the synthesized compounds

The synthesized amides underwent purification via column chromatography, and comprehensive characterization was conducted using a suite of spectroscopic techniques, including UV, IR, ^{13}C NMR, and ^{1}H NMR, as well as mass spectrometry, HPLC, and UPLC. Physico-chemical attributes such as colour, physical state, retention factor (Rf value calculated from TLC), and melting point were systematically documented.

Precoated aluminium sheets (Silica gel 60 F254, Merck Germany) were employed for thin-layer chromatography (TLC), and spots were visualized under UV light. Given the attainment of quantitative yields for amide derivatives (Compounds: 6, 10, 16, 18, and 20), the necessity for crystallization or flash column chromatographic purification (using silica gel 240–400 mesh) was obviated.

The infrared (IR) spectra of the compounds were recorded using an Agilent Cary 630 FT-IR spectrometer. Proton nuclear magnetic resonance (^{1}H NMR) and carbon-13 nuclear magnetic resonance (^{13}C NMR) spectra were acquired at ambient temperature utilizing a Bruker Spectrospin DPX-300 MHz, 400 MHz, Agilent 500 MHz FT-NMR in CDCl3 and DMSO solvent, with tetramethylsilane (TMS) serving as an internal standard. Splitting patterns denoted as s (singlet), d (doublet), t (triplet), and m (multiplet), along with chemical shift values in parts per million (ppm) and coupling constants (J) in Hertz (Hz), were ascertained.

Mass spectra were generated using a Q Star XL hybrid electron spray ionization high-resolution mass spectrometer (Applied Biosystems), covering a scan range of 100–1000 atomic mass units (amu). Melting points were determined using a digital Buchi melting point apparatus (M − 545) and recorded without correction.

2.6. Assessment of cytotoxicity assay on HepG2 cell lines

HepG2 cells were plated in a 96-well format at a density of 1.2×10^{-4} cells per well and maintained as a monolayer in DMEM without phenol red, supplemented with 10 % FCS and antibiotics (100 IU/mL of penicillin and 50 μg/mL of streptomycin) at 37 °C and 5 % CO_2 for 48 h until reaching confluency. The compounds were dissolved in DMSO at concentrations of 25, 50, 75, 100, and 125 μg. As a negative control, cells were treated with medium, with the treated groups containing an equivalent amount of DMSO. The growth-inhibitory effects of the compounds were assessed using the standard tetrazolium MTT assay.

After 48 h of incubation at 37 °C, the medium was aspirated, and 25 μL of MTT (5 mg/mL) in serum-free medium was added to each well. The plates were then incubated at 37 °C for an additional 4 h. Following incubation, the medium was removed, and 100 μL of DMSO was added to all wells. The metabolized MTT product dissolved in DMSO was quantified by measuring the absorbance at 570 nm with a reference wavelength of 655 nm using an ELISA plate reader. All assays were conducted in triplicate, and percent viability was calculated as the relative absorbance of treated cells compared to untreated control cells.

2.7. Preparation and culture of protoscolesces

Echinococcus granulosus hydatid cysts containing protoscoleces were aseptically collected from infected sheep during routine slaughter at abattoirs. The cysts, ranging from 2 to 5 cm in diameter, were dissected open, and vesicle fluid containing protoscoleces was separated from the metacestode tissue and host adventitia. Hydatid fluid, enriched with protoscoleces, was allowed to settle in 50 mL Falcon tubes at room temperature without centrifugation for 20–30 min to yield hydatid sand.

The obtained protoscoleces were washed three times in Hanks balanced salt solution (HBSS) and preserved in a sterile solution of RPMI 1640, supplemented with 12 mM HEPES, 2 mM glutamine, 200 U/mL of penicillin, 200 mg/mL of streptomycin, and 0.50 mg/mL of amphotericin B. The medium was further enriched with 10 % fetal calf serum, 4 mg/ml glucose, and phenol red. Viability and vitality of the protoscoleces were assessed using the trypan blue exclusion technique prior to any experimental procedures. A 0.01 mL solution of pooled protoscoleces was combined with 0.01 mL of 0.1 % aqueous trypan blue stain on a cavity slide and examined under low-power microscopy after 5 min.

Protoscoleces that remained unstained were classified as viable, whereas those stained with trypan blue were deemed non-viable, following the criteria established by Smyth et al. (1980). If 95 % or more of the protoscoleces were found to be viable in the sediments, the sample was deemed suitable for further experimentation.

2.8. Treatment of E. granulosus protoscoleces with amide-based compounds

The treatment of protoscoleces commenced within 10 days of initiation of the culture. A 25 ml culture flask, containing approximately 500 protoscoleces in 20 ml of culture medium, was employed for the experiment. The cultures were supplemented with varying concentrations (25, 50, 75, 100, and 125 μg/ml) of the compounds under investigation for their protoscolicidal activity. A control culture containing only DMSO was maintained for comparative purposes.

The assessment of protoscolicidal activity involved the observation of motile behavior and utilization of the trypan blue exclusion technique. All experiments were conducted in triplicate to ensure robust data analysis. Viable and non-viable protoscoleces were quantified in 10 randomly selected fields using an inverted microscope at 10X magnification. This approach provided a comprehensive

evaluation of the compounds' impact on protoscolicidal activity. For the calculation of IC50 values, nonlinear regression analysis was employed. As nonlinear regression analysis is commonly used to fit dose-response curves and aids in determining the concentration at which 50 % inhibition is achieved (IC50), the same was employed. Software package- GraphPad Prism was utilized for this purpose.

3. Results

3.1. In-silico study

The three-dimensional (3D) structures of the receptors (drug targets) were generated using the I-TASSER server. Meanwhile, the pdb files corresponding to the amide-based compounds (ligands) were prepared using ChemDraw 8.0 software (Supplementary Fig. 1). Various physico-chemical properties, such as molecular mass, the number of hydrogen bond donors and acceptors, molar refractivity,

Table 1
Docking analysis of amide-based compounds (ligands) with drug targets (receptors) of *E. granulosus*.

Sr.No.	COMPOUNDS	Docking energies (kcal/mol)			
		AQ	G_6PO_4D	FABP	Kinase
1	N-phenylbenzamide	-7.5	-7.6	-8.3	-7.6
2	3-methyl-N-p-tolylbenzamide	-7.7	-7.8	-9.2	-8.2
3	4-methyl-N-p-tolylbenzamide	-6.9	-7.9	-8.7	-8.4
4	3-nitro-N-p-tolylbenzamide	-8.5	-8.2	-9.2	-8.6
5	4-nitro-N-p-tolylbenzamide	-8.2	-7.7	-8.9	-8.6
6	***3,5-dinitro-N-p-tolylbenzamide***	-7.7	-8.5	-10.1	-8.2
7	N-p-tolylacetamide	-7.1	-6.0	-6.7	-6.3
8	2-chloro-N-p-tolylacetamide	-5.8	-7.0	-6.9	-6.3
9	2-nitro--N-p-tolylacetamide	-8.2	-8.1	-8.9	-7.8
10	***N-p-tolyl-1-naphthamide***	-8.1	-8.9	-9.9	-9.2
11	2,6-difluoro-N-p-tolylbenzamide	-8.4	-7.9	-8.9	-8.0
12	4-butyl-N-p-tolylbenzamide	-7.5	-8.0	-9.0	-8.2
13	4-tert-butyl-N-p-tolylbenzamide	-7.9	-7.9	-9.4	-8.7
14	N-p-tolyl-3,5-bis(trifluoromethyl)benzamide	-8.0	-7.8	-9.3	-9.0
15	4-methyl-3-nitro-N-p-tolylbenzamide	-7.5	-7.6	-8.5	-7.7
16	***N-p-tolyl-4-(trifluoromethoxy)benzamide***	-7.9	-8.7	-9.5	-8.8
17	4-heptyl-N-p-tolylbenzamide	-7.1	-7.9	-9.3	-8.4
18	***4-pentyl-N-p-tolylbenzamide***	-7.6	-7.8	-8.9	-8.5
19	N-p-tolyl-2-(trifluoromethyl)benzamide	-7.5	-8.2	-9.3	-8.2
20	***2,3,4,5,6-pentafluoro-N-p-tolylbenzamide***	-9.0	-9.0	-9.3	-8.5
21	*N-p*-tolylpropionamide	-8.1	-7.9	-8.2	-8.0
22	2-chloro-N-p-tolylacetamide	-5.8	-6.4	-6.6	-6.6
23	2-chloro-N-p-tolylbenzamide	-5.4	-7.8	-8.0	-7.6
24	2-chloro-N-p-tolyl-1-naphthamide	-6.6	-7.6	.-6.8	-5.8
25	2.6-dichloro-N-p-tolylbenzamide	-6.4	-5.4	-7.0	-6.8
26	4-tert-butyl-2-chloro-N-p-tolylbenzamide	-7.6	-7,8	-8.2	-9.0
27	3,5-dichloro-N-(3-chloro-4-methyphenyl) benzamide	-6.0	-5.8	-7.0	-6.8
28	*N*-(3-fluoro-4-methylphenyl)-3-nitrobenzamide	-7.8	-9.8	-7.2	-8.8
29	N-(3-chloro-4-methylphenyl)-3,5-dinitrobenzamide	-8.0	-6.6	-7.8	-8.2
30	3-chloro-N-(4-methyl-3-nitrophenyl)benzamide	-6.0	-8.2	-8.4	-8.0

Note: A color map is used for better visualization using certain threshold values of docking scores, such as derived docking scores values smaller than −8.5 kcal/mol were indicated with red color, values between −7 and −8.5 kcal/mol were colored with orange, values less than −7 kcal/mol were given in yellow color. The compounds selected for further analysis are shown in bold and italics.

Log P, molecular volume, and Weiner index, for the rationally designed library of 30 amide-based compounds were determined utilizing online drug designing tools (Supplementary Table 1).

Docking analysis of the ligands with the targeted receptors was conducted using AutoDock 4.2 (Table 1). The outcomes of the docking analysis were further scrutinized through PyMOL and LigPlot servers to elucidate the binding interactions between ligands and receptor residues. Subsequently, compounds demonstrating the most promising binding affinity against the targeted potent drug receptors of *Echinococcus* were earmarked for synthesis in the laboratory. From the initial set of 30 compounds, the top five promising candidates were selected based on docking scores obtained post-docking analysis for subsequent laboratory synthesis (Fig. 1). The compounds, identified for synthesis, include 3,5-dinitro-N-p-tolylbenzamide (Compound 6), N-p-tolyl-1-naphthamide (Compound 10), N-p-tolyl-4-(trifluoromethoxy) benzamide (Compound 16), 4-pentyl-N-p-tolylbenzamide (Compound 18), and 2,3,4,5,6-pentafluoro-N-p-tolylbenzamide (Compound 20).

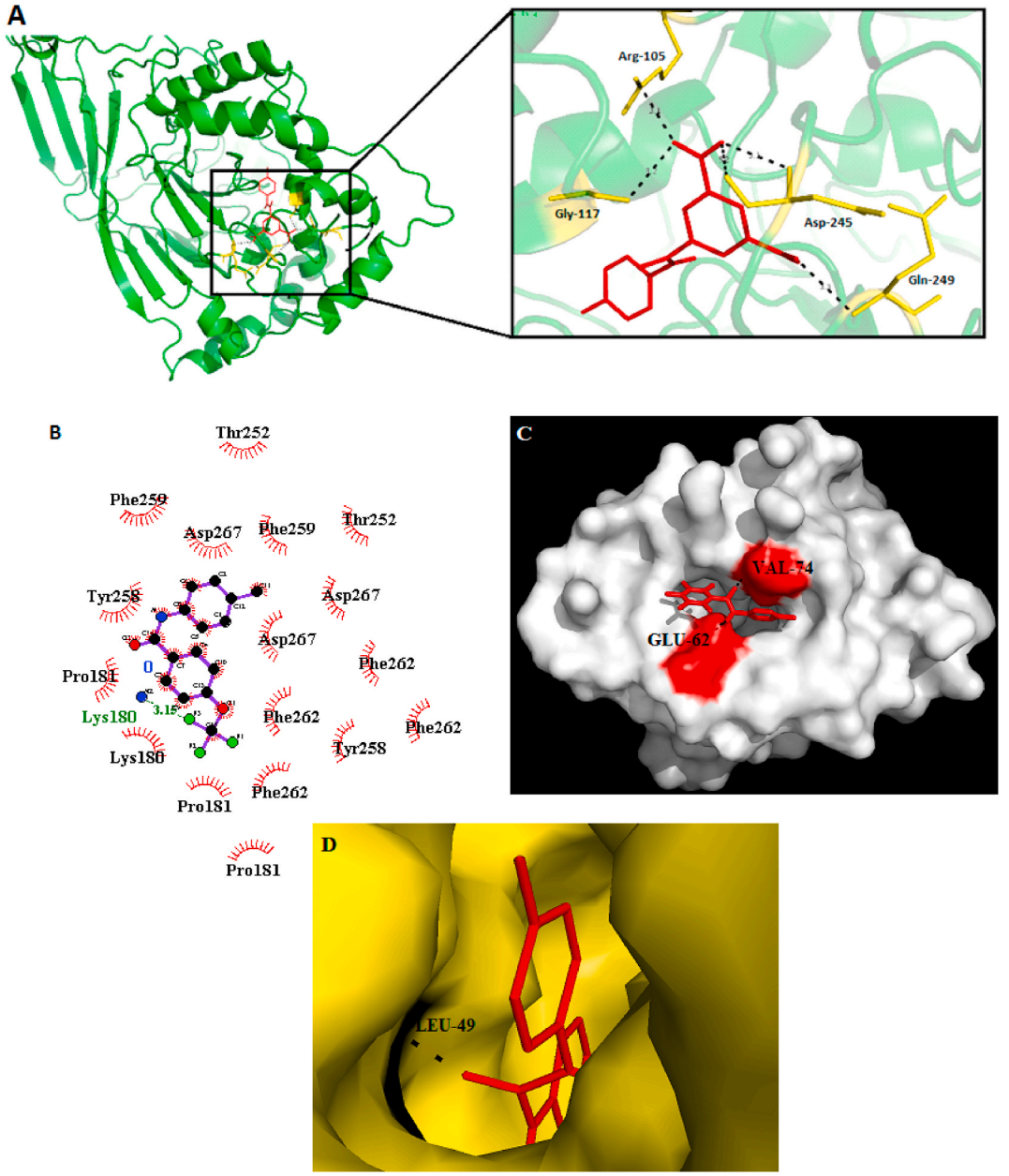

Fig. 1. (A) Binding interaction between Aquaporin and 3,5-dinitro-N-p-tolylbenzamide (Compound 6) (pymol). **(B)** Binding interaction between Glucose-6-PO_4 dehydrogenase and N-p-tolyl-4-(trifluoromethoxy) benzamide (Compound 16) (LigPlot). **(C)** Binding interaction between FABP and 2,3,4,5,6-pentafluoro-N-p-tolylbenzamide (Compound 20) in surface view. **(D)** Binding interaction between Kinase protein and N-p-tolyl-1-naphthamide (Compound 10) in surface view.

3.2. Synthesis scheme of amides (compounds 6, 10, 16, 18 and 20)

All selected compounds were synthesized chemically and were used for *in-vitro* anti-echinococcal activity as described in methodology section (Fig. 2). The physical properties of the compounds synthesized has been shown in Supplementary Table 2.

3.3. Chemistry

In this investigation, the synthesis of the aforementioned compounds was accomplished through a one-step reaction, yielding excellent results. While some of these newly synthesized benzamide derivatives have been reported previously, it's worth noting that the present synthesis employed a distinct solvent and method. The acylation process involved p-toluidine reacting with variously substituted aryl acid chlorides in the presence of acetone, with silver nanoparticles serving as a catalyst. The resultant compounds were then purified using column chromatography (Petroleum ether: ethyl acetate: 1:1), ensuring high yields, as confirmed by spectroscopic analysis. The reaction mixture, consisting of p-toluidine and diverse acid chlorides in the presence of acetone as a solvent and silver nanoparticles (5–10 nM) as a catalyst, underwent reflux for 2–3 h at 40–45^{0}C, yielding the corresponding benzamide derivatives in quantitative yields. The purity of these compounds was verified using various spectroscopic techniques, including UV, FT-IR, ^{1}H NMR, ^{13}C NMR, and mass spectrometry. The structural integrity of the newly synthesized benzamides (6, 10, 16, 18, and 20) was confirmed by their spectroscopic and analytical data.

The UV spectrum revealed an absorption peak in the wavelength region of 200–215 nm, confirming the presence of the amide group. In the IR spectrum, absorption bands within the frequency range of 1690-1630 cm-1 indicated the carbonyl stretching of amide groups, confirming the formation of benzamide derivatives. The ^{1}H NMR spectrum exhibited a sharp singlet of the amide group proton in the chemical shift range of δ 6.48–7.57 ppm, further confirming the formation of benzamide compounds (corresponding to the protons of aromatic rings should appear). Additional features such as quartet and triplet, characteristic of methyl groups in the chemical shift range of δ 3.65–4.93 ppm and δ 0.84–2.50 ppm, respectively, indicated the presence of alkyl groups in the benzene ring side chain. The ^{13}C NMR spectral data closely aligned with the assigned structures, with aromatic carbons and carbons associated with other functional groups displaying typical chemical shift values. The mass spectrum of all compounds featured molecular ion peaks and fragments, solidifying the identification of the desired compounds. The presence of either [M+H]+ or [M − H]- peaks, corresponding to their molecular formulae, was observed in all the mass spectra. Two distinct bands in the regions 1650-1687 cm^{-1} and 1510-1570 cm^{-1} in the IR spectra corroborated the presence of –CONH for C═O stretching and N–H bending vibrations, providing additional evidence for the formation of amide bonds between the substituted aryl acid chlorides and NH_2 group of p-toluidine. IR absorption bands for both aromatic and alicyclic systems were observed at their anticipated positions, demonstrating the expected influence of both electron-withdrawing and electron-releasing groups on the positions of IR peaks. The ^{13}C NMR, ^{1}H NMR, HPLC, UPLC, UV–Vis Spectroscopy and IR Spectroscopy generated for all Compounds 6, 10, 16, 18 and 20 has been shown in Supplementary Figs. 2–6.

3.4. Characterization of the synthesized compounds

3.4.1. 3,5-Dinitro-N-p-tolylbenzamide (Compound-6)

Brown solid, yield: 92 %, R_f (Petroleum ether: Ethyl acetate:1:1): 0.86, mpt: 165–168, IR: 3280, 2864, 2576, 1687, 1650, 1631, 1531, 1510, 1343, 1076, 814, 761 cm^{-1}

^{1}H NMR (400 MHz, $CDCl_3$) (δ, ppm): 9.17 (s, 3H, Ar–H, CH), 7.48 (d, 4H, J = 1.6Hz, Ar–H, CH), 6.98 (s, 1H, NH), 2.12 (q, 3H, J = 1.6Hz, CH_3), ^{13}C NMR (125 MHz, DMSO-d_6): 20.6, 120.8, 121.4, 128.0, 129.2, 130.0, 148.2 ppm, HR-MS: for $C_{14}H_{11}N_3O_5$ $[M+H]^+$ calculated 301.25 *m/z*, found 300.1 *m/z*.

3.4.2. N-p-tolyl-1-naphthamide (Compound-10)

Mint cream solid, yield: 95 %, R_f (Petroleum ether: Ethyl acetate:1:1): 0.86, mpt: 144–146, IR: 3226, 3037, 2918, 2577, 1655, 1601, 1531, 1512, 1324, 1261, 782, 748 cm^{-1}

^{1}H NMR (400 MHz, $CDCl_3$) (δ, ppm): 8.94 (s, 1H, CH), 8.35 (s, 1H, NH), 7.51 (d, 10H, J = 3.2 Hz, Ar–H, CH), 2.34 (t, 3H, J = 20 Hz, CH_3), ^{13}C NMR (125 MHz, DMSO-d_6): 20.4, 20.6, 30.8, 119.8, 125.1, 125.4, 126.4, 129.2, 130.2, 167.1 ppm, HR-MS: for $C_{18}H_{15}NO$ $[M+H]^+$ calculated 261.32 *m/z*, found 262.4 *m/z*.

3.4.3. N-p-tolyl-4-(trifluoromethoxy)benzamide (Compound-16)

Wheat coloured solid, yield: 94 %, R_f (Petroleum ether: Ethyl acetate:1:1): 0.83, mpt: 194–196, IR: 3321, 2568, 2579, 1652, 1601, 1531, 1516, 1207, 1162, 812, 773, 713 cm^{-1}

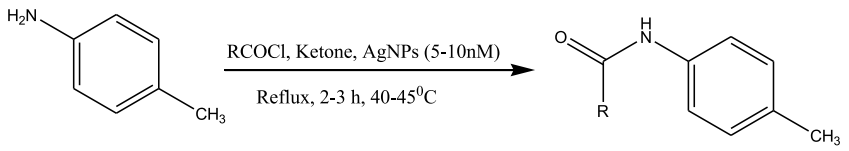

Fig. 2. Chemical Reaction showing strategy applied for the synthesis of amide-based compounds. Where R = 3,5-bis-nitrophenyl (6), 1-naphthalene (10), 4-trifluoromethoxyphenyl (16), 4-pentylphenyl (18), 2,3,04,5,6-pentafluorophenyl (20).

^{1}H NMR (400 MHz, $CDCl_3$) (δ, ppm): 8.07 (s, 1H, NH), 7.59 (d, 6H, $J = 12.0$ Hz, Ar–H, CH), 7.36 (q, 2H, $J = 2.0$ Hz, Ar–H, CH), ^{13}C NMR (125 MHz, DMSO-d_6): 20.4, 20.6, 120.7, 122.6, 129.1, 130.0, 130.2, 134.2, 136.5, 149.7, 150.4, 156.3, 164.2 ppm, HR-MS: for $C_{15}H_{12}F_3NO_2$ $[M+H]^+$ calculated 295.26 *m/z*, found 296.4 *m/z*.

3.4.4. 4-Pentyl-N-p-tolylbenzamide (Compound-18)

Burly wood coloured solid, yield: 93 %, R_f (Petroleum ether: Ethyl acetate:1:1): 0.87, mpt: 138–140, IR: 3330, 2920, 2861, 1648, 1613, 1598, 1516, 1406, 1320, 814, 752, 672 cm^{-1}

^{1}H NMR (400 MHz, $CDCl_3$) (δ, ppm): 9.73 (s, 1H, NH), 7.31 (d, 6H, $J = 8.0$ Hz, Ar–H, CH), 7.23 (q, 2H, $J = 8.0$ Hz, Ar–H, CH), 2.57 (d, 2H, $J = 4.0$ Hz, Ar–H, CH_2), 0.87 (t, 3H, $J = 6.8$ Hz, CH_3), ^{13}C NMR (125 MHz, DMSO-d_6): 20, 30, 34, 120.4, 127.7, 128.3, 129.0, 130.2, 133, 147, 167 ppm, HR-MS: for $C_{19}H_{23}NO$ $[M+H]^+$ calculated 281.39 *m/z*, found 282.3 *m/z*.

3.4.5. 2,3,4,5,6-Pentafluoro-N-p-tolylbenzamide (Compound-20)

Saddle brown solid, yield: 91 %, R_f (Petroleum ether: Ethyl acetate:1:1): 0.84, mpt: 182–185,
IR: 3257, 3196, 3060, 2581, 1721, 1672, 1605, 1553, 1499, 1335, 992, 812, 715 cm^{-1}

^{1}H NMR (500 MHz, DMSO-d_6) (δ, ppm): 10.17 (s, 1H, Ar–H, NH), 7.25–7.25 (d, 2H, $J = 8.0$ Hz, Ar–H, CH), 7.23 (q, 2H, $J = 4.0$ Hz, Ar–H, CH), 2.48 (q, 3H, $J = 4.0$ Hz, CH_3), ^{13}C NMR (125 MHz, DMSO-d_6): 119.6, 122.9, 129.5, 130.1, 130.2, 133.9, 135.6, 137.0, 154.7, 154.7 ppm, HR-MS: for $C_{14}H_8F_5NO$ $[M+H]^+$ calculated 301.21 *m/z*, found 300.2 *m/z*.

3.5. In-vitro cytotoxicity assay of the synthesized compounds by using human hepatic cancer cell line (HepG2 cell line)

The *in-vitro* cytotoxicity assessment of the synthesized compounds was conducted using the standard MTT protocol on the human hepatic cancer cell line (HepG2). A sub-confluent population of HepG2 cells was exposed to escalating doses of the tested compounds, and the count of viable cells was observed after a 3-day incubation period. All five compounds were examined across a concentration range of 25, 50, 75, 100, and 125 μg/ml. Remarkably, 4-pentyl-N-p-tolylbenzamide (Compound 18) demonstrated the least cytotoxicity on HepG2 cell lines, with a cell survival rate of approximately 54 % on the third day at a concentration of 125 μg/ml. Following this, N-p-tolyl-1-naphthamide (Compound-10), N-p-tolyl-4-(trifluoromethoxy)benzamide (Compound-16), 3,5-dinitro-N-p-tolylbenzamide (Compound-6) and 2,3,4,5,6-pentafluoro-N-p-tolylbenzamide (Compound-20) exhibited a 40 %, 38 %, 36 % and 32 % survival rate, respectively. Despite varying degrees of cytotoxicity, all five compounds demonstrated substantial efficacy (viability percentage of cell growth) within the specified concentration range (Fig. 3).

3.6. Scolicidal activity of amide derivatives

The viability of *E. granulosus* protoscoleces following treatment with varying concentrations of all five synthesized compounds was recorded. No significant differences were observed in the survival rate of protoscoleces in the control group even after 5 days. The scolicidal activity of all five compounds were observed as follows:

3.6.1. 3,5-Dinitro-N-p-tolylbenzamide (compound 6)

The viability of protoscoleces after treatment with 3,5-dinitro-N-p-tolylbenzamide at concentrations of 25, 50, 75, 100, and 125 μg/ml was observed as 72.6 %, 66.6 %, 53.6 %, 43 %, and 32.3 %, respectively, on the fifth day. These results suggest that the compound exhibits limited effectiveness against *E. granulosus* protoscoleces, necessitating a higher dose for protoscolicidal activity

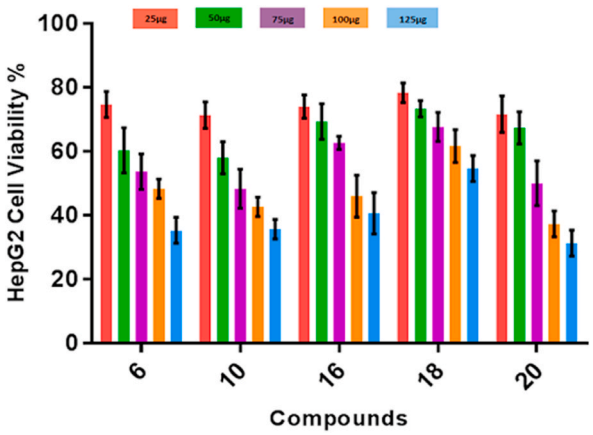

Fig. 3. Graph depicting the survival rate of HepG2 cell lines with different concentrations (25, 50, 75, 100 and 125 μg/ml) of all five compounds. Compounds **6:** 3,5-dinitro-N-p-tolylbenzamide, **10:** N-p-tolyl-1-naphthamide, **16:** N-p-tolyl-4-(trifluoromethoxy) benzamide, **18:** 4-pentyl-N-p-tolylbenzamideand, **20:** 2,3,4,5,6-pentafluoro-N-p-tolylbenzamide).

(Supplementary Fig. 7).

3.6.2. N-p-tolyl-1-naphthamide (compound 10)

The viability of protoscoleces after treatment with N-p-tolyl-1-naphthamide at concentrations of 25, 50, 75, 100, and 125 μg/ml was observed as 47.3 %, 20 %, 10.3 %, 0 %, and 0 %, respectively, on the fifth day. This study suggests that the compound is highly effective against *E. granulosus* protoscoleces, exhibiting profound protoscolicidal activity within five days (Fig. 4).

3.6.3. N-p-tolyl-4-(trifluoromethoxy) benzamide (compound 16)

The viability of protoscoleces after treatment with N-p-tolyl-4-(trifluoromethoxy) benzamide at concentrations of 25, 50, 75, 100, and 125 μg was observed as 72.6 %, 62.6 %, 45.3 %, 39.6 %, and 30 % on the fifth day. The results suggest that the compound is effective against protoscoleces at slightly higher concentrations (Supplementary Fig. 8).

3.6.4. 4-Pentyl-N-p-tolylbenzamide (compound 18)

The viability of protoscoleces after treatment with 4-pentyl-N-p-tolylbenzamide at concentrations of 25, 50, 75, 100, and 125 μg was observed as 63.3 %, 49.6 %, 38.3 %, 29 %, and 21 % on the fifth day. The results suggest that the compound is effective against protoscoleces at higher concentrations (Supplementary Fig. 9).

3.6.5. 2,3,4,5,6-Pentafluoro-N-p-tolylbenzamide (compound 20)

The viability of protoscoleces after treatment with 2,3,4,5,6-pentafluoro-N-p-tolylbenzamide at concentrations of 25, 50, 75, 100, and 125 μg was observed as 54.3 %, 50.6 %, 18.3 %, 9.6 %, and 0 % on the fifth day. The results suggest that the compound possesses profound protoscolicidal activity (Supplementary Fig. 10).

3.7. Half-maximal inhibitory concentration

The compound N-p-tolyl-1-naphthamide demonstrated the lowest IC_{50} value at 29.51 μg/ml, indicating potent protoscolicidal activity. Following closely were 2,3,4,5,6-pentafluoro-N-p-tolylbenzamide with an IC50 of 39.55 μg/ml, N-p-tolyl-4-

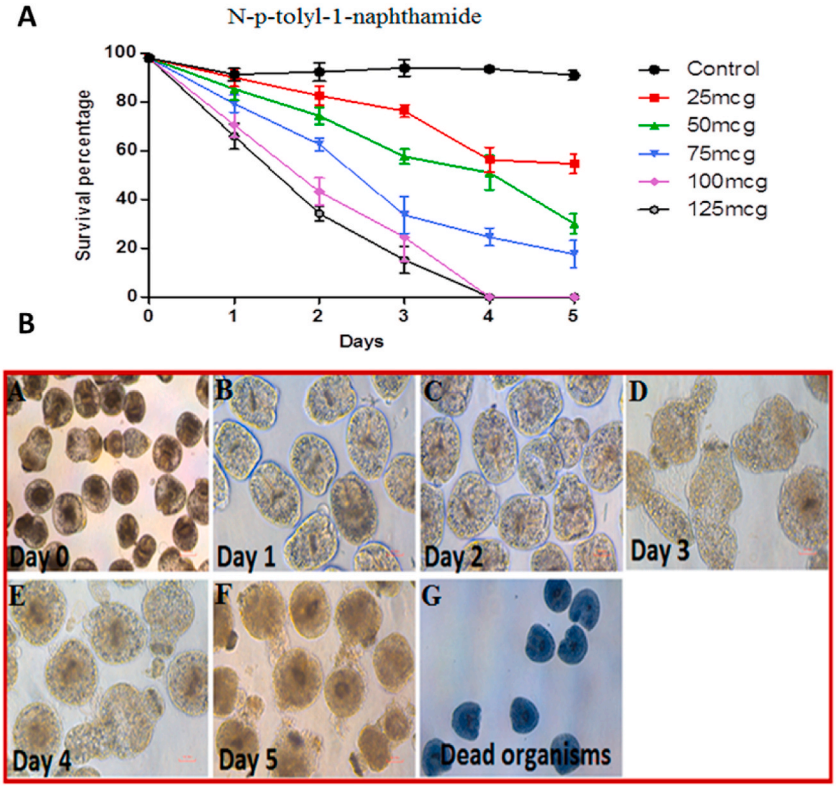

Fig. 4. (A) Graph depicting the viability percentage of *E. granulosus* protoscolesces on treatment with N-p-tolyl-1-naphthamide at different concentrations for five consecutive days. **(B)** Showing the effect on protoscolesces after treatment with N-p-tolyl-1-naphthamide. A-F- Shows the morphological changes in protoscolesces from day 0 to day 5. Note the disorganized protoscolesces on day 4th and 5th. G- Trypan Blue staining on day fifth- The dead cells are stained blue and the live cells remained unstained. (For interpretation of the references to colour in this figure legend, the reader is referred to the Web version of this article.)

(trifluoromethoxy) benzamide with an IC_{50} of 66.51 μg/ml, 4-pentyl-N-p-tolylbenzamide with an IC50 of 44.98 μg/ml, and 3,5-dinitro-N-p-tolylbenzamide with an IC50 of 77.02 μg/ml (Fig. 4.75). In summary, N-p-tolyl-1-naphthamide (compound 10) emerged as the most potent protoscolicidal agent in this study, followed by 2,3,4,5,6-pentafluoro-N-p-tolylbenzamide (compound 20), N-p-tolyl-4-(trifluoromethoxy) benzamide (compound 16), 4-pentyl-N-p-tolylbenzamide (compound 18), and 3,5-dinitro-N-p-tolylbenzamide (compound 6) (Fig. 5).

4. Discussion

The treatment of Cystic Echinococcosis (CE) primarily involves radical resection of the parasitic mass, accompanied by chemotherapy [19]. In cases where surgery is not viable, chemotherapy becomes the sole option, with Albendazole and Mebendazole being the current drugs of choice [20]. However, the use of these drugs poses challenges, including adverse effects [21]. Consequently, there is a pressing need to explore novel anti-echinococcal agents to effectively combat this life-threatening disease. It's noteworthy that the field of anti-echinococcal drug discovery has seen limited exploration compared to other parasitic infections like *Schistosoma*, *Trypanosoma*, *Toxoplasma*, *Leishmania*, and *Plasmodium* [22]. Amide-based compounds have demonstrated promising antiparasitic activity. Nitazoxanide, an amide derivative, exhibited potent antiechinococcal activity against protoscoleces and metacestodes of *Echinococcus granulosus* [23]. Similarly, Al-Qtaitat et al. [24], reported the antimalarial, antileishmanial and antischistosomal activity of novel metronidazole-piperazine amides. Draper et al. [25], reported Pyridyl ethyl amides as potential antitrypanosomal agents, and arylimidamide-azole hybrids as potential antileishmanial agents. Smit et al. [26], reported the antimalarial activity of novel 4-amino-quinolinyl-chalcone amides. These studies suggest the feasibility of treating Echinococcosis with such compounds.

Silver nanoparticles have garnered interest in various fields due to their unique properties, including high surface area-to-volume ratio and catalytic activity. In the context of our study, the incorporation of AgNPs in the synthesis process may have facilitated the formation of amide bonds through several possible mechanisms. AgNPs are known to exhibit catalytic activity by providing active sites for chemical reactions, promoting the coupling of carboxylic acids and amines to form amide bonds. Additionally, AgNPs could act as electron acceptors, facilitating the transfer of electrons during the reaction process, thereby enhancing the efficiency of the amidation reaction. While the precise mechanistic details of AgNPs' involvement in the amidation process were not explored in our study, their inclusion likely contributed to the efficiency and selectivity of the synthesis method. Future investigations could focus on elucidating the specific mechanisms by which AgNPs catalyze the formation of amide bonds, potentially through spectroscopic and kinetic studies [27,28].

The current study aimed to investigate the therapeutic potential of a library of 30 amide-based compounds against CE, utilizing both *in-silico* and *in-vitro* approaches (Fig. 6). *In-silico* analysis involved the rational design of these compounds, virtual screening against *E. granulosus* drug targets, and subsequent molecular docking studies. Selected drug targets included Aquaporin 4, Kinase A, Fatty Acid Binding Protein, and Glucose-6-Phosphate-1-Dehydrogenase due to their crucial roles in the parasite's survival and proliferation [20]. In the bioinformatics results, all 30 compounds underwent molecular docking analysis, and structure-activity relationship (SAR) analysis was conducted. The parameters like molecular weight, binding affinity, molar volume, molar refractivity, lipophilicity, number of hydrogen bond donors or hydrogen bond acceptors and Weiner index etc.) which influence the physico-chemical properties of the drug molecules were analyzed for all the compounds. These physico-chemical descriptors signify numerical values that characterize properties of drug molecules and influence biological activity (receptor binding) to a certain extent. Several studies on different drug molecules have been reported which depicted that physico-chemical (especially lipophilicity logP) and electronic (e.g. binding affinity) properties exhibit a significant influence on biological activity [29,30]. Various physico-chemical

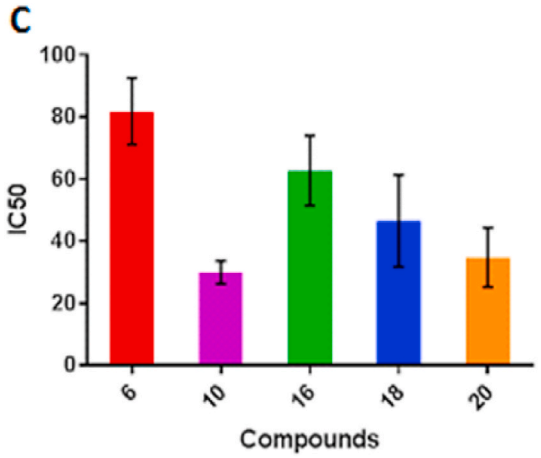

Fig. 5. IC_{50} values of all the five compounds. 3,5-dinitro-N-p-tolylbenzamide (Compound 6), N-p-tolyl-1-naphthamide (compound 10), N-p-tolyl-4-(trifluoromethoxy) benzamide (Compound 16), 4-pentyl-N-p-tolylbenzamide (compound 18), 2,3,4,5,6-pentafluoro-N-p-tolylbenzamide (compound 20).

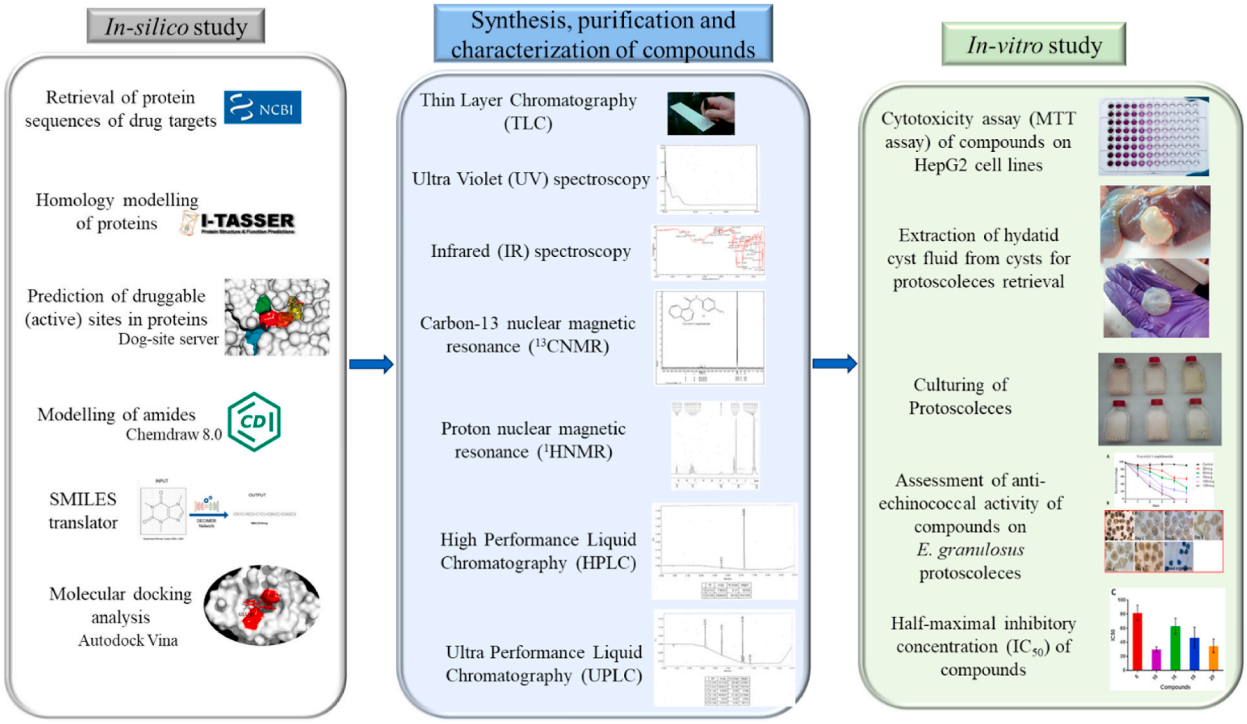

Fig. 6. Pictorial representation of the overall methodology adopted in the study.

and electronic parameters were considered, revealing that compounds with lower predicted lipophilicity values were within the acceptable limits of Lipinski's rule of five, indicating good membrane permeating inhibitors. In context of drugs properties, lipophilicity has been studied and practiced for decades, since most of the drugs permeate biological membranes via passive transport which depends on their lipophilicity (logP) to a huge extent. The top five compounds (6, 10, 16, 18, and 20) exhibiting the highest affinities with drug targets were selected for further analysis.

Moving on to wet lab results, these five compounds were synthesized and characterized using various techniques including UV–vis spectroscopy, IR spectroscopy, HPLC, UPLC, ^{13}C NMR, ^{1}H NMR, and mass spectrometry, ensuring their structural integrity. *In-vitro* cytotoxicity assays on HepG2 cell lines demonstrated varying degrees of cytotoxicity, with Compound 18 displaying the least cytotoxicity, making it a potential candidate for further investigation. Protoscolicidal activity was also assessed, with Compound 10 emerging as the most effective, showing a rapid and profound impact on protoscoleces viability. We targeted protoscolesces in place of metacestodes of *Echinococcus*, as protoscolesces not only have the ability to develop into adult tapeworms in intestine of intermediate host but are also capable to differentiate into metacestodes on reaching different organs. The study highlighted the significance of lipophilicity and electronic properties in influencing anti-echinococcal activity. The results indicated that para- and meta-substituted benzamides or non-substituted N-p-tolyl-1-naphthamide exhibited higher antiechinococcal activity than ortho-substituted compounds. Moreover, the parameters impacting antiechinococcal activity may include lipophilicity and electronic (e.g. binding affinity) properties of the individual substituents. It is worthwhile to mention that the inhibitory effects against *E. granulosus* strain enhanced with higher logP values (lipophilicity) and also electron-withdrawing groups are more useful than electron donor groups. Normally, it can be illustrated that from all the five tested compounds para- and meta-substituted benzamides or non-substituted N-p-tolyl-1-naphthamide (compound 10) showed higher antiechinococcal activity than ortho-substituted compounds. This is probably due to a steric effect of a spatially-close group. The spatial proximity of the ortho-substituent to the amide group on the p-toluidine ring induces a twist in the aniline ring plane, orienting it towards the amide group and, consequently, the entire naphthalene core. On the other hand, meta- and particularly para-substitution tends to favor a planar structure. In cases where the substituent is more lipophilic, this planar arrangement facilitates easy permeation through various biological membranes, as demonstrated by Malik et al. [31]. Thus, the lipophilicity of meta- and para-substituted benzamides was resulted to be the major factor responsible for anti-echinococcal activity of such structures. Because the compounds with electron-withdrawing groups represented anti-echinococcal activities, it can be pointed out that these components affecting electronic density (charge) at the carbonyl group impact the potential of binding of the amide group to possible binding sites in an echinococcal cell.

In the future, further investigations could expand upon this study's findings by exploring additional structural modifications of the synthesized compounds to enhance their anti-echinococcal efficacy. Specifically, focusing on optimizing the substituents and functional groups within the amide-based compounds may lead to the development of more potent and selective agents against cystic echinococcosis. Additionally, conducting in vivo studies using animal models would provide valuable insights into the pharmacokinetic and pharmacodynamic profiles of the most promising compounds, thereby advancing their preclinical development.

Furthermore, exploring potential synergistic effects of the synthesized compounds with existing anti-parasitic drugs could offer novel combination therapies with enhanced efficacy against Echinococcus granulosus. Finally, considering the evolving landscape of drug discovery, leveraging computational techniques such as molecular dynamics simulations and quantitative structure-activity relationship (QSAR) modeling may further elucidate the underlying mechanisms of action and optimize the design of future anti-echinococcal agents.

5. Conclusion

The integration of computational and experimental methods in drug discovery is a notable strength of this study. The rational design of compounds based on *in-silico* predictions followed by their synthesis and *in-vitro* validation demonstrates a systematic and efficient drug discovery pipeline. N-p-tolyl-1-naphthamide (Compound 10) was identified as the most promising candidate. The findings support further evaluation of these compounds in animal models to assess their *in-vivo* efficacy and safety profiles. Additionally, the study contributes to the growing body of knowledge on neglected tropical diseases and highlights the importance of interdisciplinary approaches in drug discovery. While *in-silico* predictions provide a valuable starting point, experimental validation is essential to confirm the actual efficacy of the compounds. The *in-vitro* model using HepG2 cell lines and protoscoleces provides a preliminary assessment. Further studies should include animal models to better simulate the *in-vivo* environment. The translation of findings from bench to bedside requires additional studies, including pharmacokinetics, pharmacodynamics, and safety assessments in human subjects. In conclusion, this study contributes to the ongoing efforts in developing novel therapeutic strategies for Cystic Echinococcosis. The integration of computational and experimental approaches enhances the robustness of the findings, setting the stage for further investigations towards potential drug candidates for clinical applications.

Limitations of the study

There is limited existing research specifically focusing on the anti-echinococcal activity of amide-based compounds. While studies on antimalarial, antileishmanial, and antischistosomal activities have been conducted with similar nature of compounds (as discussed in discussion section), the differences in target proteins and tested compounds make direct comparisons challenging. However, due to the unique nature of our study, direct comparisons with these findings are not feasible.

Funding

Not applicable.

Institutional review board statement

Not applicable.

Informed consent statement

Not applicable.

Consent for publication

All the authors have read and approved the manuscript and all are aware of its submission to the journal.

Code availability

Not applicable.

Ethics approval

Approved by Institution Ethical Committee (IEC) no: SUBMS/IEC/10/52.

Data availability statement

All data are available in this manuscript.

CRediT authorship contribution statement

V. Chauhan: Writing – review & editing, Writing – original draft, Software, Methodology, Investigation, Formal analysis, Data curation, Conceptualization. **U. Farooq:** Writing – review & editing, Supervision, Project administration, Investigation, Data curation, Conceptualization. **M.K. Fahmi:** Writing – review & editing, Project administration, Conceptualization. **Khan A:** Software, Project

administration, Methodology, Investigation, Formal analysis, Data curation. **P.K. Tripathi:** Writing – original draft, Validation, Resources, Methodology, Formal analysis, Data curation.

Declaration of competing interest

There is no conflict among the author's.

Acknowledgments

The authors would like to acknowledge Deanship of graduate study and Scientific Research Taif University for funding this work.

Appendix A. Supplementary data

Supplementary data to this article can be found online at https://doi.org/10.1016/j.heliyon.2024.e31205.

References

[1] V. Chauhan, A. Khan, U. Farooq, In silico study to predict promiscuous peptides for immunodiagnosis of cystic echinococcosis, Tropenmed. Parasitol. 13 (1) (2023) 54–62, https://doi.org/10.4103/tp.tp_70_22.
[2] L. Omadang, M. Chamai, F. Ejobi, J. Erume, P. Oba, M. Ocaido, Prevalence of cystic echinococcosis among livestock in pastoral and agro-pastoral areas in Uganda, Parasitology 28 (2023) 1–9, https://doi.org/10.1017/S0031182023001154.
[3] B. Chen, M. Yan, H. Gao, et al., In vitro and in vivo efficacies of novel harmine derivatives in the treatment of cystic echinococcosis, Drug Des. Dev. Ther. 17 (2023) 2441–2454, https://doi.org/10.2147/DDDT.S419002.
[4] G. Umhang, C. Richomme, V. Bastid, J.M. Boucher, C.P. de Garam, S. Itié-Hafez, C. Danan, F. Boué, National survey and molecular diagnosis of Echinococcus granulosus sensu lato in livestock in France, 2012, Parasitology 147 (6) (2020) 667–672.
[5] V.P. Bhalla, S. Paul, E. Klar, Hydatid disease of the liver, Visc. Med. 39 (5) (2023) 112–120, https://doi.org/10.1159/000533807.
[6] W. Zhang, J. Li, D. Liu, Immunological prophylaxes for Echinococcus granulosus infection, Inmolecular Medical Microbiology 1 (2024) 3205–3220. Academic Press.
[7] P.S. Craig, D. Hegglin, M.W. Lightowlers, P.R. Torgerson, Q. Wang, Echinococcosis: control and prevention, Adv. Parasitol. 96 (2017 January 1) 55–158, https://doi.org/10.1016/bs.apar.2016.09.002.
[8] H. Wen, L. Vuitton, T. Tuxun, et al., Echinococcosis: advances in the 21st century, Clin. Microbiol. Rev. 32 (2) (2019 March 20) 10–128, https://doi.org/10.1128/CMR.00075-18.
[9] G.R. Silveira, K.A. Campelo, G.R.S. Lima, et al., In vitro anti-Toxoplasma gondii and antimicrobial activity of amides derived from cinnamic acid, Molecules 23 (4) (2018 March 28) 774, https://doi.org/10.3390/molecules23040774.
[10] M.A. da Silva, H.H. Fokoue, S.N. Fialho, et al., Antileishmanial activity evaluation of a natural amide and its synthetic analogs against Leishmania (V.) braziliensis: an integrated approach in vitro and in silico, Parasitol. Res. 120 (6) (2021 June) 2199–2218, https://doi.org/10.1007/s00436-021-07169-w.
[11] P.J. Dornbush, C. Cho, E.S. Chang, et al., Preliminary studies of 3, 4-dichloroaniline amides as antiparasitic agents: structure-activity analysis of a compound library in vitro against Trichomonas vaginalis, Bioorg. Med. Chem. Lett 20 (17) (2010 September 1) 5299–5301, https://doi.org/10.1016/j.bmcl.2010.06.133.
[12] L.D. Mendelsohn, ChemDraw 8 ultra, windows and macintosh versions, J. Chem. Inf. Comput. Sci. 44 (6) (2004 November 22) 2225–2226, https://doi.org/10.1021/ci040123t.
[13] C.A. Lipinski, Lead-and drug-like compounds: the rule-of-five revolution, Drug Discov. Today Technol. 1 (4) (2004 Dec 1) 337–341, https://doi.org/10.1016/j.ddtec.2004.11.007.
[14] X. Zhou, W. Zheng, Y. Li, et al., I-TASSER-MTD: a deep-learning-based platform for multi-domain protein structure and function prediction, Nat. Protoc. 17 (10) (2022 October) 2326–2353, https://doi.org/10.1038/s41596-022-00728-0.
[15] A. Volkamer, D. Kuhn, F. Rippmann, M. Rarey, DoGSiteScorer: a web server for automatic binding site prediction, analysis and druggability assessment, Bioinformatics 28 (15) (2012 August 1) 2074–2075, https://doi.org/10.1093/bioinformatics/bts310.
[16] O. Trott, A.J. Olson, AutoDock Vina: improving the speed and accuracy of docking with a new scoring function, efficient optimization, and multithreading, J. Comput. Chem. 31 (2) (2010 January 30) 455–461, https://doi.org/10.1002/jcc.21334.
[17] I. Sondi, B. Salopek-Sondi, Silver nanoparticles as antimicrobial agent: a case study on E. coli as a model for Gram-negative bacteria, J. Colloid Interface Sci. 275 (1) (2004 Jul 1) 177–182.
[18] N. Durán, P.D. Marcato, O.L. Alves, G.I. De Souza, E. Esposito, Mechanistic aspects of biosynthesis of silver nanoparticles by several Fusarium oxysporum strains, J. Nanobiotechnol. 3 (2005 Jul) 1–7.
[19] A. Erfani, R. Shahriarirad, M. Eskandarisani, M. Rastegarian, B. Sarkari, Management of liver hydatid cysts: a retrospective analysis of 293 surgical cases from Southern Iran, J. Trop. Med. 19 (2023 June) 9998739, https://doi.org/10.1155/2023/9998739.
[20] M. Ibrahim, A.W.M. Jobran, A. Attalah, I. Abassi, M.B.A. Isneineh, A primary hydatid cyst in the mesorectum uncommon location–A rare case report, Int J Surg Case Rep 114 (2024 January 1) 109061, https://doi.org/10.1016/j.ijscr.2023.109061.
[21] R.T. Zewude, A. Corbeil, S. Fung, C.A. Moulton, I.I. Bogoch, Alveolar Echinococcus in a 70-year-old man in Ontario, J Assoc Med Microbiol Infect Dis Can 8 (4) (2024 January 16) 336–342, https://doi.org/10.3138/jammi-2023-0012.
[22] H. Zheng, W. Zhang, L. Zhang, et al., The genome of the hydatid tapeworm Echinococcus granulosus, Nat. Genet. 45 (10) (2013 October) 1168–1175, https://doi.org/10.1038/ng.2757.
[23] M. Walker, J.F. Rossignol, P. Torgerson, A. Hemphill, In vitro effects of nitazoxanide on Echinococcus granulosus protoscoleces and metacestodes, J. Antimicrob. Chemother. 54 (3) (2004 September 1) 609–616, https://doi.org/10.1093/jac/dkh386.
[24] M.A. Al-Qtaitat, H.A. Saadeh, A.G. Al-Bakri, et al., Synthesis, characterization, and biological activity of novel metronidazole-piperazine amides, Monatsh. Chem. 146 (4) (2015 April) 705–712, https://doi.org/10.1007/s00706-014-1352-0.
[25] Draper J. Synthesis of Pyridyl Ethyl Amides as Potential Antitrypanosomal Agents, and Synthesis of Arylimidamide-Azole Hybrids as Potential Antileishmanial Agents..
[26] F.J. Smit, D.D. N'da, Synthesis, in vitro antimalarial activity and cytotoxicity of novel 4-aminoquinolinyl-chalcone amides, Bioorg. Med. Chem. 22 (3) (2014 February 1) 1128–1138, https://doi.org/10.1016/j.bmc.2013.12.032.
[27] M. Rai, A. Yadav, A. Gade, Silver nanoparticles as a new generation of antimicrobials, Biotechnol. Adv. 27 (1) (2009 Jan 1) 76–83.
[28] X.F. Zhang, Z.G. Liu, W. Shen, S. Gurunathan, Silver nanoparticles: synthesis, characterization, properties, applications, and therapeutic approaches, Int. J. Mol. Sci. 17 (9) (2016 Sep 13) 1534.

[29] M. Millard, J. Kilian, M. Ozenil, et al., Design, synthesis and preclinical evaluation of muscarine receptor antagonists via a scaffold-hopping approach, Eur. J. Med. Chem. 262 (2023 December 15) 115891, https://doi.org/10.1016/j.ejmech.2023.115891.
[30] M. Huynh, R. Vinck, B. Gibert, G. Gasser, Strategies for the nuclear delivery of metal complexes to cancer cells, Adv. Mater. 4 (2024 January) e2311437, https://doi.org/10.1002/adma.202311437.
[31] M.S. Malik, S.A. Ahmed, I.I. Althagafi, M.A. Ansari, A. Kamal, Application of triazoles as bioisosteres and linkers in the development of microtubule targeting agents, RSC Med. Chem. 11 (3) (2020) 327–348, https://doi.org/10.1039/c9md00458k.